J. Am. Chem. Soc. 1981, 103, 4378-4381

Low-Temperature EPR Studies of Highly Anisotropic Low-Spin (Protoporphyrinato)iron(III) Complexes

Catharina T. Migita and Masamoto Iwaizumi*

Contribution from the Chemical Research Institute of Non-Aqueous Solutions, Tohoku University, Sendai 980, Japan. *Received August 11, 1980*

Abstract: Low-spin complexes of ferric protoporphyrin IX showing highly anisotropic EPR spectra (HALS) have been investigated by systematically changing the axial bases. From EPR measurements at low temperatures, complete sets of principal g values were obtained for a series of these complexes. The cubic field strength and tetragonal splitting in these HALS complexes appear to be smaller than those of ordinary low-spin complexes (LS). Interestingly, the tetragonal splitting of HALS complexes decreases with an increase of the axial field strength, in contrast to that of LS complexes where the tetragonal splitting increases with an increase of the axial field strength. From an analysis of the ligand field parameters obtained from the HALS complexes it has been suggested that the ferric ions in the HALS complexes may be a little displaced from the porphyrin plane and also that the HALS state may be close to the spin-crossover point between the intermediate-spin and the high-spin states.

Ferric porphyrins produce well-known low-spin complexes with axial ligands such as imidazole, cyanide, azide, thiols, and phenoxide, which show EPR spectra quite characteristic of the low-spin type.[1] According to the ligand field analysis developed by Peisach and Blumberg,[1a,c] these low-spin complexes have a tetragonal splitting greater than two (in units of spin-orbit coupling constant) and the ferric ions are under an effective D_4 ligand field. To a good approximation the ground spin state of these complexes is considered to be in the $t_{2g}{}^5$ configuration.[2] In this paper we denote these typical low-spin complexes, LS for short.

On the other hand, some of these heme-ligand complexes exhibit very large g anisotropy, although they are still classified as low-spin species (denoted by HALS, hereafter). Because of extreme broadening of the EPR signals at the high field side, complete spectra cannot be observed in most cases. Hence, a complete analysis of the spectra and systematic studies has not been reported on such ferric complexes.[3,4] Denatured heme proteins such as denatured cytochrome c are examples which yield highly anisotropic EPR signals.[5] However, because of the lack of knowledge of the three g values, reliable information about magnetic and electronic states of the ferric ions has not been obtained. Clearly, the observation of the complete EPR spectra of these species is the principal requirement for the investigation of these complexes.

The main purpose of the present research is to establish how the electronic state and the structure of heme complexes are affected by the changes of axial ligand field in the low-spin domain, and we have observed that a series of the ferric porphyrin complexes show the HALS EPR spectra on coordination with some weak nitrogen heterocyclic bases.

The investigation of such HALS complexes is interesting in relation to the spin-state transformation of the heme iron, because, as discussed later, the HALS state, may be close to the spin-crossover point between the high-spin and the low-spin states or between the low-spin and intermediate-spin states.

Table I. Classification of N Bases According to the Specific Type of Complexes $Fe^{III}(PPIX)\cdot(N\ base)_n$, ($n$ = 1 or 2)[a]

HS	HS and HALS	HALS	HALS and LS	LS	
2-NH_2py triazine	4-CN(py) 2-Me(py) 3-Me(py) 1,4-diazine 1,3-diazine 1,2-diazine quinoline	py 4-Me(py) 3-NH_2py	4-NH_2py		six-membered ring base
		BzIm 2-MeIm	3-MePz	Im N-MeIm 4-MeIm Pz triazole	five-membered ring base

[a] For abbreviations, see ref 7.

For the HALS complexes we could observe the spectral features of a sharp peak and two broad peaks corresponding to the three principal g values. Based on the systematic data obtained from the g values, we attempted a ligand field analysis following Taylor's method.[6] The resultant ligand field parameters for these HALS complexes exhibited some differences from the parameters in the more typical LS complexes.

Experimental Section

(Protoporphyrin IX ato)iron(III) chloride [Fe^{III}(PPIX)Cl] was used as purchased from Sigma. (Octaethylporphyrinato)iron(III) [Fe^{III}(OEP)Cl] was synthesized from ferrous sulfate and free base OEP obtained from Nakarai Chemical.

Methylene chloride, *N,N*-dimethylformamide (DMF), and dimethyl sulfoxide (Me_2SO) were used as solvents and were from Uvasol. All the heterocyclic nitrogen bases (N bases)[7] were of reagent grade and were purified by sublimation or vacuum distillation, if necessary. Caution was taken to keep the reagents dry.

Solutions of the complexes were prepared by dissolving the iron porphyrins into CH_2Cl_2 solutions of liquid N bases. When the N bases are solid, a minimum amount of DMF or Me_2SO was added to the CH_2Cl_2 to aid in dissolving the iron(III) porphyrins and the N bases. Silver

---

(1) (a) Chance, B., Ed. "Probes of Structure and Function of Macromolecules and Membranes"; Academic Press: New York, 1971; Vol. II. (b) Dorphin, D., Ed. "The Porphyrins"; Academic Press: New York, 1979; Vol. IV Chapters 6-9. (c) Peisach, J.; Blomberg, W. E.; Adler, A. *Ann. N.Y. Acad. Sci.* **1973**, *206*, 310-327. (d) Scoller, D. M.; Hoffman, B. M. *J. Am. Chem. Soc.* **1979**, *101*, 1655-1662. (e) Hori, H. *Biochim. Biophys. Acta* **1971**, *251*, 227-235. (f) Shalman, R. G.; Glarum, S. H.; Karplus, M. *J. Mol. Biol.* **1971**, *57*, 93-115. (g) La Mar, G. N.; Walker, F. A. *J. Am. Chem. Soc.* **1973**, *95*, 1782-1790. (h) Tang, S. C.; Koch, S.; Papaefthymiou, G. C.; Foner, S.; Frankel, R. B.; Ibers, J. A.; Holm, R. H. *Ibid.* **1976**, *98*, 2414-2434. (i) Ainscough, E. W.; Addison, A. W.; Dorphin, D.; James, B. R. *Ibid.* **1978**, *100*, 7585-7591. (j) Chevion, M.; Peisach, J.; Blumberg, W. E. *J. Biol. Chem.* **1977**, *252*, 3637-3645. (k) Ruf, H. H.; Wende, P. *J. Am. Chem. Soc.* **1977**, *99*, 5499-5500.

(2) (a) Otsuka, J. *J. Phys. Soc. Jpn.* **1966**, *21*, 596-620. (b) *Ibid.* **1968**, *24*, 885-910. (c) Weissbluth, M. "Structure and Bonding"; Springer-Verlag: New York, 1967; Vol. 2, pp 1-125. (d) Bohan, T. L. *J. Magn. Reson.* **1977**, *26*, 109-118.

(3) (a) Mims, W. B.; Peisach, J. *J. Chem. Phys.* **1976**, *64*, 1074-1091. (b) Rhynard, D.; Lang, G.; Spartalian, K. V. *Ibid.* **1979**, *71*, 3715-3721.

(4) Hill, H. A. O.; Morallee, K. G. *J. Am. Chem. Soc.* **1972**, *94*, 731-738.

(5) Brautigan, D. L.; Feinberg, B. A.; Hoffman, B. M.; Margoliash, E.; Peisach, J.; Blumberg, W. E. *J. Biol. Chem.* **1977**, *252*, 574-582.

(6) Taylor, C. P. S. *Biochim. Biophys. Acta* **1977**, *491*, 137-149.

(7) The abbreviations for the N bases are as follows: pyridine, py; methylpyridine, Me(py); aminopyridine, NH_2py; cyanopyridine, CN(py); imidazole, Im; methylimidazole, MeIm; benzimidazole, BzIm; Pyrazole, Pz; methylpyrazole, MePz.

0002-7863/81/1503-4378$01.25/0

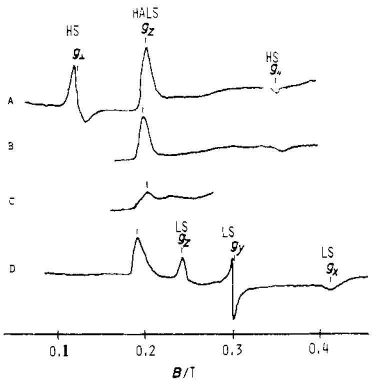

Figure 1. EPR spectra of HS, HALS, and LS obtained from some N-base complexes: (A) 2-Me(py) complexes at 9.7 K, (B) 4-Me(py) complex at 10 K and (C) at 41.5 K, (D) 4-NH$_2$py complex at 9.5 K. A signal from quartz interferes at the $g_\parallel$ position (see also Figures 2 and 6).

nitrate was used to exchange nitrate for chloride.

Sampling was performed on a vacuum line by using a sample tube connected to a high quality quartz EPR tube. Reaction residues were filtered with a glass filter set between the sample and the EPR tube.

The porphyrin concentration was kept at or below 1×10^{-3} M to prevent aggregation of the porphyrins. Base concentration was adjusted so as to range from a few to a thousand times the porphyrin concentration.

EPR spectra were measured on a Varian E-112 X-band spectrometer equipped with tapered ring-shim tips and with an Oxford EPR 9 or 10 cryostat. The former cryostat was for measurements above 4 K and the latter for those below 4 K. The microwave frequencies were monitored by Takedariken TR 5501 frequency counter with a TR 5023 frequency converter.

Experimental Results

The complexes of ferric protoporphyrin IX with N bases examined in our experiments can be classified into three types on the basis of their EPR features (Table I): typical high-spin complexes with g values of 6 and 2 (HS), low-spin complexes (LS), and highly anisotropic low-spin complexes (HALS). In the formation of the base adducts, some bases produce both the HS and HALS complexes while others produce a mixture of HALS and LS complexes. In the former cases, the HALS complexes are assigned to the bis(N-base) adducts and the HS to the monobase adducts. When Me$_2$SO (or DMF) is present as a component of the mixed solvents, the HS may be assigned to the mixed bisadducts of N base and Me$_2$SO (or DMF). Meanwhile, in the latter cases, the LS complexes are assigned to the bis(N-base) adducts and the HALS to the mono(N-base) adducts or to the mixed bisadducts of N base and Me$_2$SO (or DMF) when these compounds are present in the reaction system. When a large excess of pyridine was used as a N base, only the HALS complexes was formed, but when a molar equivalent of pyridine was added to the ferric porphyrins, only the HS complex was formed. This indicates that the HALS species of the pyridine adduct is a bis(pyridine) complex. The other N-base adducts which gave only the HALS species may be in the bis(N-base) adducts as in the case of the pyridine complex. As Table I shows, stronger bases generally tend to produce the LS rather than the HALS complexes or the HALS rather than the HS complexes. However, bases with substituents sterically hindered for coordination apparently reduce this tendency substantially. It is also seen that the five-membered ring bases generally have a high tendency to form the LS complexes. In view of these observations, it can be considered that the HALS is formed by an axial perturbation intermediate in magnitude between that for HS and that for LS and the cubic field strength in the HALS is between those in the HS and LS complexes.

The HALS complexes also exhibit characteristic in stabilities; the EPR signal of some of the complexes drastically decreased within a few days while those for the others completely disappeared when the solutions were kept at room temperatures. This implies that the HALS complexes may be less stable than the HS and LS species. Reduction of the ferric ion by the N bases may also occur.

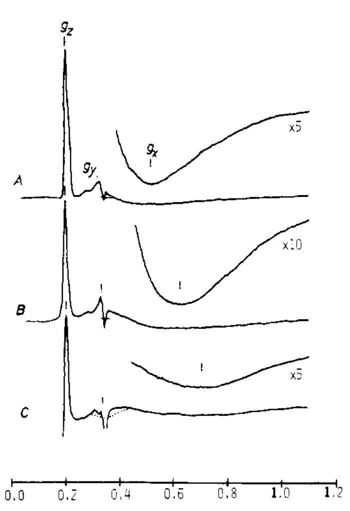

Figure 2. EPR spectra of some HALS complexes at 2 K: (A) the BzIm complex; (B) the 2-MeIm complex; (C) the 2-Me(py) complex.

Examples of the EPR spectra of the HS, HALS, and LS are illustrated in Figure 1. At the temperatures used for the measurements of these EPR spectra, only one peak was detected for the HALS species. However, when temperatures were lowered below 2 K, whole spectra for the HALS became detectable but the peaks at the high field side were still very broad and the highest wings of the spectra extended to 1 T. Some examples of the spectra are shown in Figure 2. In the series of the HALS complexes, the minimum g value varied markedly with the N bases.

In addition to exhibiting a larger g anisotropy the HALS EPR spectra exhibited several diagnostic features in comparison with LS spectra. All the HALS spectrum signals become undetectable above 45 K, while the LS signals were detected even above 77 K. The $g_{\max}$ peak of HALS spectra was temperature dependent;[8] as the temperature increased, $g_{\max}$ became smaller, whereas the three g values of the LS complexes remained nearly constant over the temperature range of 9–77 K. Furthermore, the EPR spectra of the HALS complexes are harder to saturate with microwave power than are the spectra of the LS series; the LS signals were saturated by a microwave power of 15 mW at 10 K, but the HALS samples must be cooled to 2 K for saturation of the EPR signals by the same microwave power.

In this work, Fe$^{\text{III}}$(OEP) as well as Fe$^{\text{III}}$(PPIX) were examined. No intrinsic differences were observed in both systems, but the HALS complexes of Fe$^{\text{III}}$(OEP) gave a slightly larger g anisotropy.

Discussion

The Ligand Field Analysis for the HALS and LS Complexes. Using the complete sets of the g values for the HALS and LS, we have the ligand field analysis, according to Taylor's method.[6]

The ground-state Kramers doublet is expressed by formula 1,

$$|+\rangle = a|d_{yz}^{+}\rangle - ib|d_{zx}^{+}\rangle - c|d_{xy}^{-}\rangle$$

$$|-\rangle = -a|d_{yz}^{-}\rangle - ib|d_{zx}^{-}\rangle - c|d_{xy}^{+}\rangle \qquad (1)$$

where a, b, and c are real numbers. The principal g values represented in terms of the wave function coefficients are given in eq 2. When orbital reduction due to covalent bonding with ligands

$$g_z = 2[(a+b)^2 - c^2]$$

$$g_y = 2[(a+c)^2 - b^2]$$

$$g_x = 2[a^2 - (b+c)^2] \qquad (2)$$

---

[8] Temperature dependence of the other g components could not be examined because they become undectable on elevation of temperature.

Table II. g Values, Coefficients, and Ligand Field Parameters for HALS and LS Complexes with Five-Membered Ring N Bases

axial ligand	g_z	g_y	g_x	a	b	c	Σ^a	V/λ	Δ/λ	$\lvert V/\Delta \rvert$	type of complex
Im	2.91	2.24	1.53	0.957	0.256	0.132	0.999	1.92	3.44	0.558	LS
4-MeIm	2.86	2.25	1.56	0.961	0.245	0.128	0.999	2.04	3.43	0.594	LS
N-MeIm	2.92	2.25	1.52	0.957	0.259	0.135	1.001	1.90	3.34	0.568	LS
triazole	2.97	2.17	1.30	0.927	0.301	0.157	0.975	1.55	2.89	0.537	LS
BzIm	3.40	2.40	1.27	0.963	0.354	0.188	1.089	1.35	2.55	0.529	HALS
2-MeIm	3.48	2.36	1.05	0.943	0.393	0.212	1.089	1.15	2.26	0.504	HALS
3-MePz^b	2.7										HALS?

^{a} $\Sigma = a^2 + b^2 + c^2$. ^{b} Only one signal was observed, and the saturation behavior and the temperature dependence of the signal were similar to those of the HALS.

Table III. g Values, Coefficients, and Ligand Field Parameters for HALS and LS Complexes with Six-Membered Ring Bases

axial ligand	g_z	g_y	g_x	a	b	c	Σ	V/λ	Δ/λ	$\lvert V/\Delta \rvert$	type of complex
4-NH$_2$py^a	2.83	2.27	1.63	0.968	0.228	0.121	1.004	2.21	3.64	0.608	LS
1,4-diazine^b	3.23										HALS
1,2-diazine	3.29	2.24	1.25	0.945	0.349	0.169	1.045	1.32	2.89	0.459	HALS
4-CN(py)	3.25	2.25	1.10	0.927	0.362	0.194	1.028	1.25	2.40	0.519	HALS
Py	3.43	2.25	0.98	0.926	0.400	0.207	1.061	1.09	2.33	0.469	HALS
3-Me(py)	3.48	2.28	0.98	0.931	0.404	0.210	1.075	1.08	2.31	0.469	HALS
1,3-diazine	3.31	2.44	1.23	0.956	0.346	0.201	1.074	1.39	2.26	0.615	HALS
2-Me(py)	3.41	2.24	0.94	0.920	0.402	0.212	1.054	1.07	2.25	0.476	HALS
quinoline^b	3.48										HALS
3-NH$_2$py	3.48	2.40	0.78	0.921	0.423	0.253	1.090	1.02	1.77	0.577	HALS
4-Me(py)	3.46	2.42	0.81	0.923	0.416	0.253	1.089	1.05	1.76	0.597	HALS
4-NH$_2$py^a	3.58	2.49	0.78	0.933	0.430	0.263	1.125	1.02	1.71	0.594	HALS

^{a} The complex in the LS state is 2(4-NH$_2$py) complex, while the one in the HALS state is the mixed ligand complex of 4-NH$_2$py and DMF. ^{b} The higher field signals of these complexes were undetectable because of their weak intensity.

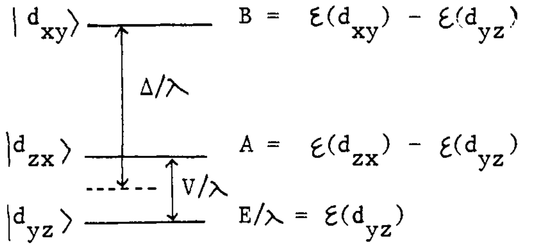

Figure 3. Hole state energies and ligand field parameters for t_{2g}^5 configuration, where $|\,\rangle$ represents a state and $E(\ )$ the state energy and λ is the spin–orbit coupling constant.

is negligible, the squared sum $\sum = a^2 + b^2 + c^2$ is unity. Using these wave functions, we solved the eigenvalue equation (3). Here,

$$(-\lambda)\cdot\begin{pmatrix} 0 & i/2 & -1/2 \\ -i/2 & -A & i/2 \\ -1/2 & -i/2 & -B \end{pmatrix}\cdot\begin{pmatrix} a \\ -ib \\ -c \end{pmatrix} = E\cdot\begin{pmatrix} a \\ -ib \\ -c \end{pmatrix} \qquad (3)$$

the energy of the lowest Kramers doublet E is set to the energy of the d_{yz} orbital. A and B correspond to the relative energies of the d_{zx} and d_{xy} orbitals to the d_{yz} (see Figure 3); they are given by eq 4, where λ is the absolute value of the spin–orbit coupling

$$E/\lambda = -(b + c)/2a = g_x/(g_z + g_y) - \tfrac{1}{2}$$

$$A = E/\lambda + (a + c)/2b = g_x/(g_z + g_y) + g_y/(g_z - g_x)$$

$$B = E/\lambda + (a + b)/2c = g_x/(g_z + g_y) + g_z/(g_y - g_x) \qquad (4)$$

parameter, whose negative sign has been included explicitly in the equations. The ligand field parameters defined in Figure 3 are defined as $V/\lambda = A$ and $\Delta/\lambda = B - (A/2)$.

In this analysis, assignment of the g values to the principal axis system and their sign is made so as to satisfy the following requirements: $g_xg_yg_z > 0$, $g_z + g_y - g_x > 0$, and $V/\Delta < {}^2/_3$. Here, the x and y axes are taken to be in the porphyrin plane and z is normal to the plane.

The derived wave function coefficients and ligand field parameters are listed in Tables II and III together with the experimental g values obtained at 2 K. In these tables, the complexes are arranged in the order of decreasing Δ/λ value.

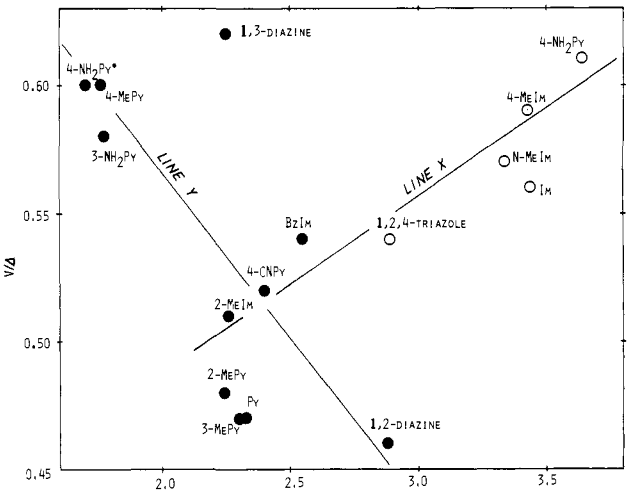

Figure 4. V/Δ vs. Δ/λ plot for HALS (●) and LS (○) complexes. All the complexes are bisbase adducts except for the asterisked complex.

We mentioned before that the cubic field strength in the HALS complexes appeared to be weaker than that in the LS complexes. It can also be seen from these tables that the relation between the field strength of axial bases and tetragonal splitting Δ/λ is quite different in the HALS and LS series. That is, stronger field ligands give a larger tetragonal splitting in the LS series, while the stronger field ligands result in smaller tetragonal splitting in the HALS series. For example the bis(imidazole) complex (LS) has a Δ/λ of 3.44 and bis(triazole) complex (LS) has a value of 2.89, whereas the bis(4-methylpyridine) complex (HALS) has a Δ/λ of 1.71 and bis(4-cyanopyridine) complex has a value of 2.40. The axial field strength in the bis(triazole) and bis(1,2-diazine) complexes is on the border of those in the HALS and LS complexes. However, as will be explored later, the magnitude of the tetragonal splitting itself is not necessarily the best parameter to distinguish the HALS state from the LS state. Figure 4 shows the correlation between the rhombicity V/Δ and the tetragonal splitting Δ/λ. The Δ/λ and V/Δ apparently exhibit a positive

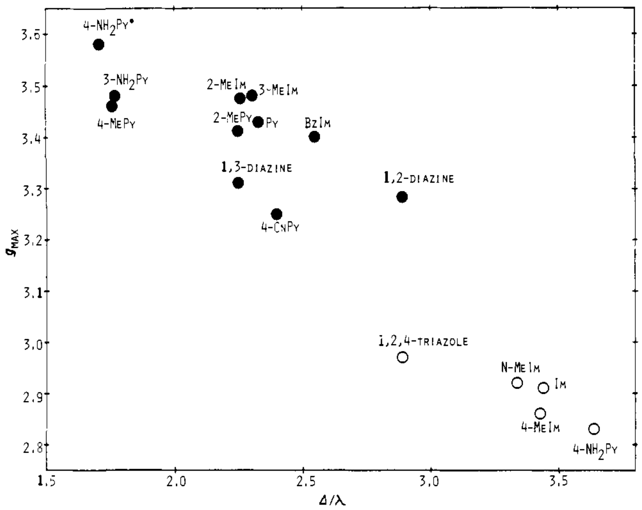

Figure 5. g_{max} vs. Δ/λ plot for HALS (●) and LS (○) complexes. All the complexes are bisbase adducts except for the asterisked complex.

correlation in the LS series (line X) but a negative correlation in the HALS series (line Y).

The axial field affects the t_{2g} levels in the following three ways: (a) electrostatic repulsion between the electrons in the iron d_{yz} and d_{zx} orbitals and the axial ligand orbitals; (b) change in the π-bond interaction between the metal d_{yz} and d_{zx} orbitals and the porphyrin in-plane π orbitals; (c) displacement of the ferric ion from the porphyrin least square plane. The first effect would destabilize the metal d_{yz} and d_{zx} orbitals more and provide a larger tetragonal separation when stronger axial bases are added. If the in-plane anisotropy is mainly caused by the axial ligand interaction with specific orientation with respect to the porphyrin plane, they would also give a larger rhombicity.

It has been shown by NMR studies that porphyrin-to-metal charge transfer (CT) is more effective in complexes of the weaker base.[4,9] This means that a decrease in d_{yz} and d_{xz} destabilization by a weakening of axial field would be partly compensated by an increase in metal d_{yz} and d_{zx} electron density owing to the effective CT (the second effect).

On the other hand, the third effect would stabilize the d_{xy} orbital and destabilize the d_{yz} and d_{zx} orbitals. The larger contribution of c would result in the larger Δ/λ value. The first two effects on d_{yz} and d_{zx} orbitals explain well the observed results in the LS series. In the case of the HALS series, the observed unique relation between the axial ligand strength and ligand field parameters cannot be explained with only these two effects. Rather it appears that the ferric ion in the HALS complexes is displaced from the porphyrin plane and the interaction with the stronger bases at the fifth and sixth positions reduces this displacement, so that the Δ/λ values become smaller. The temperature dependence observed for g_{max} in the HALS complexes suggests that the interaction of the N bases with the ferric porphyrins weakens as the temperature increases and the ferric ion is displaced more from the porphyrin plane.

As is apparently seen from Tables II and III, the V/λ values in the HALS complexes are much smaller than those obtained with LS complexes. Furthermore, the decrease of the V/λ values is less than that of the Δ/λ values in the HALS series, so that the V/Δ vs. Δ/λ relation yields a negative slope (line Y, Figure 4). Such scanty variation in the V/λ values with the axial base in the HALS series implys that the specific orientation of the axial ligand to the porphyrin ring cannot make the main contribution to the observed rhombicity any longer because of the weak field strength of the axial base. Jahn–Teller distortion of the porphyrin ring may be responsible for the in-plane anisotropy.

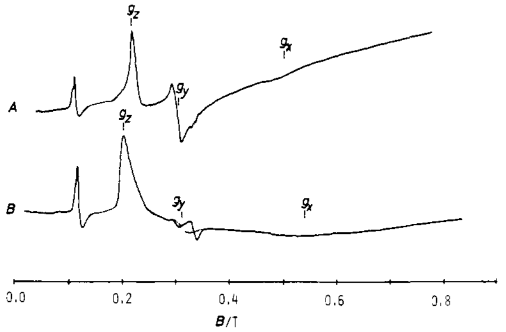

Figure 6. Comparison of the EPR spectral feature of LS originated from bis(triazole) complex (A) with that of HALS from the 1,2-diazine complex (B) measured at 2 K.

Correlation between g_{max} and Δ/λ. In the EPR spectra of the HALS complexes only the g_z ($=g_{max}$) peak is conspicuous when spectra are recorded above 10 K. Therefore, it seems valuable to examine whether or not g_{max} is a useful parameter for estimating the magnitude of the tetragonal splitting. Figure 5 presents a plot of g_{max} vs. Δ/λ for the HALS and LS series. A negative correlation is found but the correlation is fairly small among the HALS group, indicating that g_{max} will not necessarily provide correct information about the Δ/λ value. The tetragonal splittings estimated from the g_{max} values for the cytochromes by Brautigan et al.[5] do not fit with the slope shown in Figure 5, though these cytochromes seem to belong to the HALS category since their g_{max} values reside around 3.4.

Conclusive Remarks. As already mentioned, several EPR features distinguish the HALS from LS. One of the most distinctive features is that the HALS complexes show large g anisotropy, corresponding to the small tetragonal splitting, than is found in ordinary LS complexes. This small splitting is attributed to the weaker axial field strength in HALS complexes than that in LS complexes. However, the characteristics of the HALS EPR spectrum cannot be explained simply by the smallness of Δ/λ. For example, the 1,2-diazine and triazole complexes are clearly distinctive in the EPR features (see Figure 6), belonging to different groups in spite of their almost identical Δ/λ values. Changes in the field strength by different axial ligands affect both the cubic splitting and the tetragonal splitting in a different way. Among the HALS series, the cubic splitting decreases monotonously with decreasing axial field strength but the tetragonal splitting increases. This effect is in vivid contrast to the effect of axial ligands on the tetragonal splitting in the LS complexes, where the tetragonal splitting decreases with a decrease of the axial field strength. The increase of the tetragonal splitting with the decrease in the axial field strength in the HALS complexes can be satisfactorily explained by assuming that the ferric ion is displaced more from the porphyrin plane by the interaction with the weaker N bases. As already mentioned the HALS complexes have smaller cubic splitting. The excited states, where d_{z^2} and $d_{x^2-y^2}$ orbitals participate, will therefore contribute more to the HALS ground state. Such electronic state can be close to the intermediate-spin state[9] of $(d_{xy})^2(d_{yz},d_{zx})^2(d_{z^2})^1$ or to the HS state.

In the above discussion, we have treated the HALS complexes by assuming the pure $t_{2g}{}^5$ configuration. However, the fact that the e_g levels may be situated closer to t_{2g} levels suggests that the $t_{2g}{}^5$ approximation may be barely usable in the HALS system, as is suspected from the relatively large deviation from unity of $a^2 + b^2 + c^2$ (Tables II and III). The higher excited state may have to be taken into account for a more quantitative discussion of the HALS state.

---

[9] Goff, H.; Shimomura, E. *J. Am. Chem. Soc.* **1980**, *102*, 31–37.